Indian Journal of Pure & Applied Physics
Vol. 61, August 2023, pp. 683-691
DOI: 10.56042/ijpap.v61i8.806

Room Temperature Ammonia Sensing of MoS_2 2D Sheets Decorated with Polyaniline (PANI)

Ali Akbar[a], Mausumi Das[b] & D Sarkar[a]*

[a]Department of Physics, Gauhati University, Guwahati 781 014, Assam, India
[b]Department of Physics, Sipajhar College, Sipajhar 784 145, Assam, India

Received 26 April 2023; accepted 14 July 2023

In the present work, a selective room temperature (RT) operable ammonia (NH_3) sensor based on molybdenum disulphide (MoS_2) nanosheet decorated with polyaniline (PANI) (MoS_2-PANI) is successfully developed. The sensor material is prepared by simple chemical in-situ polymerisation of aniline**.** Prior to the gas sensing studies, morphological, thermal and compositional studies are carried out. These studies reveal good incorporation of PANI into MoS_2 nanosheets. The gas sensing property of MoS_2-PANI sensors is studied and compared with the sensor based on bare MoS_2 and bare PANI. The bare PANI shows opposite gas sensing properties compared to the bare MoS_2. However, the sensing nature of PANI is followed in the composite, but with better sensing and stability. The sensing behaviour is observed to be excellent in terms of stability, selectivity, sensitivity, response and recovery over the pure MoS_2 sensor.

Keywords: Molybdenum disulphide; Polyaniline; Composites; Ammonia sensing; Selectivity; Repeatability.

1 Introduction

There has been rapid enhancement of hazardous contribution of gases to the environment due to the rapid development of industries. Among various hazardous gases, ammonia (NH_3) is recognised as one of the major polluting gases. Exposure to even very low concentrations of NH_3 can cause irritation to the eyes, nose, and throat and also contribute to various respiratory disorders[1-5]. The maximum time of exposure notified by the Occupational Safety and Health Administration (OSHA) in a workplace, for 25 ppm and 35 ppm NH_3 to be 8 h and 15 min, respectively[6]. The human body also produces NH_3 naturally through various metabolic activities[7]. In the health sector, the presence of high concentrations of NH_3 in exhaled human breath indicates diseases related to the liver and kidneys[8]. Hence, there is an urgent need to develop, ideally, a reliable low cost and highly sensitive gas sensor system to detect NH_3 at room temperature.

Conducting polymers (CPs) are well known to a category of low-cost and RT-operated sensing materials[9,10]. Polyaniline (PANI), among this category, is the most used CPs due to its easy synthesis technique, environmental stability and reversible redox reaction in the field of RT gas sensing[11,12]. However, these detectors based on CPs are often found to suffer from a lack of stability and exhibit poor sensitivity because of the huge affinity of these polymers towards other volatile organic compounds (VOCs) and dew present in the environment[13,14]. The gas sensor is based on inorganic materials, for example, tungsten oxide (WO_2), zinc Oxide (ZnO), tin oxide (SnO_2), titanium oxide (TiO_2), iron oxide (Fe_2O_3), silicon oxide (SiO_2) etc., show enhanced detecting qualities, but at the same time, they are efficient at high temperatures (300−400 °C), which requires high power and consequently can shorten the lifetime of the device[15-20]. So, on the one hand, there are organic CPs which are operative at room temperature but face issues regarding stability, selectivity etc., and on the other hand, there are inorganic materials which solve the latter issues but are operative at temperatures much higher than the ambient. So, the issues can be overcome by utilising composites of these two categories of materials to develop an efficient and stable gas sensor which can be operational at ambient temperature.

Nowadays, a new class of 2D MoS_2 nanomaterial has fascinated great attention among researchers in developing suitable gas sensors due to its wide electrical properties and planar arrangement of atomic thin layered nanostructures[21-25]. In recent years, PANI-based nanocomposite gas sensors have been

*Corresponding authors:
(E-mail: sarkardeepali@gmail.com)

successfully developed and utilised by several research groups to detect hazardous NH_3 at ambient conditions. Kulkarni *et al.*[26] reported NH_3 gas/vapour sensor based on hybrid polyaniline (PANI)-WO_3 composites using *an in-situ* chemical oxidative polymerisation technique. Bandgar *et al.*[27] developed a PANI-Fe_2O_3 nanocomposite-based NH_3 sensor, exhibiting the highest response of 39% to 100 ppm NH_3 gas. Also, to mention work from the present group itself [28] to develop a CdS-PANI NH_3 sensor for efficient detection at room temperature. Some reports on the ammonia sensing performance of polyaniline and its nanocomposites with organic/inorganic materials are also available in the literature [29-33]. Zhang *et al.*[34]demonstrated ternary nanocomposites based on polyaniline with multi-walled carbon nanotubes and molybdenum disulphide and its high-performance ammonia sensing at room temperature. The works available in the literature, along with the expertise of the present group in the field, have motivated the authors to develop a suitable room temperature-operated NH_3 sensor based on MoS_2-PANInanocomposite.

The present work reports the development of an NH_3 gas sensor based on the MoS_2-PANI nanocomposite. The composite is prepared by simple and low-cost in-situ chemical dispersion polymerisation technique. The obtained response of the as-prepared composite film in terms of sensitivity (S%) is relatively high, with other reported works on NH_3 sensing by PANI-MoS_2 composite. The recovery of the sensor is significantly improved without using any external appliances. The gas sensing results of the MoS_2-PANI sensor fabricated by this method might be advantageous to develop an efficient room temperature operable NH_3 detector.

2 Experimental

2.1 Materials used

The materials that have been used for the present investigation are ammonium heptamolybdate tetrahydrate [$(NH_4)_6MO_7O_{24}{\cdot}4H_2O$], citric acid ($C_6H_8O_7$), thiourea ($CH_4N_2S$), ammonium persulphate (APS), aniline (C_6H_7N) and dodecyl benzene sulphonic acid (DBSA). Ammonium heptamolybdate tetrahydrate [$(NH_4)_6MO_7O_{24}{\cdot}4H_2O$], citric acid ($C_6H_8O_7$), and thiourea ($CH_4N_2S$) are purchased from Merck Life Science Private Limited. Ammonium persulphate (APS) is obtained from Fisher Scientific, aniline (C_6H_7N) from SD Fine Chemicals Limited and dodecyl benzene sulphonic acid (DBSA) from Sigma-Aldrich. Aniline is distilled repeatedly prior to every use. Deionised water is used throughout as the solvent medium of the reaction.

2.2 Methodology

2.2.1 Synthesis of MoS_2

The ammonium heptamolybdate tetrahydrate, citric acid, and thiourea (CH_4N_2S) are utilised as the potential elements and the sulphur source to obtain MoS_2[35]. Typically, 1.5g of ammonium heptamolybdate tetrahydrate and 0.5g of citric acid are dissolved in deionised water under vigorous magnetic stirring and kept at 90 °C for 30 min. The ammonia solution is added to the above-mentioned solution to maintain the PH value of the solution at 4. Then, a solution of thiourea (1.3g) in water is added drop-wise to this solution under vigorous stirring. Finally, the composite solution is transferred to a 40 ml Teflon lined steel autoclave and kept at 120 °C for 8 hrs. The black precipitate that is obtained is collected by centrifugation and filtration. The obtained precipitate is washed repeatedly with deionised water and ethanol and dried at 90 °C and preserved for any measurements to be carried out.

2.2.2 Synthesis of MoS_2-PANI Nanocomposites

Typically, 0.25g of MoS_2 is dispersed in 20 ml of 1M aq. HCL solution and sonicate it for 3 hrs to get a uniform MoS_2 dispersion. In another beaker, polyaniline is prepared by chemical polymerisation technique, as has been discussed in some earlier work [28]. Synthesis of MoS_2-PANI nanocomposites is done in the same bath of preparation of PANI. Typically, 10 ml of DBSA (0.1M) and aniline (0.1M) in 1M aq. (HCl) the solution is stirred separately for 30 minutes. Then the combined solution is stirred in an ice bath for another 1 hr, and APS (0.25M) in 10 ml of aqueous HCL is added to the combined solution. MoS_2 dispersion is added to the polyaniline synthesis bath and stirred for another 2 hrs, and the resultant solution is kept in the refrigerator for 8 hrs. Finally, the obtained composite dispersion is filtered and washed with deionised water and ethanol and dried at room temperature. Then films of the materials are made by spin coating their dispersions at 600 rpm.

2.3 Characterisation Techniques

The morphology of the materials is investigated by employing field emission secondary electron microscopy (FESEM; Model: Zeiss sigma -300). Thermal analyses are recorded by a Mettler Toledo: TGA 2. The Fourier Transform Infrared Spectroscopy

(FTIR) studies are done using a spectrophotometer (Model: Perkin Elmer Spectrum 1000). The conductometric mode of gas sensing measurements is recorded by measuring the change in electrical resistance on the incorporation of gas using a Keithley 2400 source meter equipped with a computer interface. The schematic of the gas sensing set-up for the measurement of change in resistance of the as-prepared films is shown in Fig. 1.

3 Results and Discussion

3.1 FESEM Study

Figure 2 shows the morphology of MoS_2, PANI and MoS_2-PANI composite, respectively. Fig. 2(a) shows a FESEM picture of MoS_2, which reveals a smooth surfaced 2D nanosheet single-layer structure of thickness of a few nanometres and lateral dimensions of 2.37 µm, Fig. 2(b) shows a FESEM image of pure PANI, which displays a collection of nanofibers. From the FESEM of MoS_2-PANI composites (Fig. 2(c & d)), nanofiber-like structures of PANI are seen to be distributed over MoS_2nanosheets. This result reflects that PANI has been successfully polymerised on the surface of the MoS_2nanosheet via a simple chemical dispersion polymerisation technique. Moreover, some small pore-like structures are also observed in the FESEM images of both pure and composite films. The decoration of PANI on the surface of MoS_2-supplied active sites, which might offer MoS_2-PANI a suitable, efficient gas sensor.

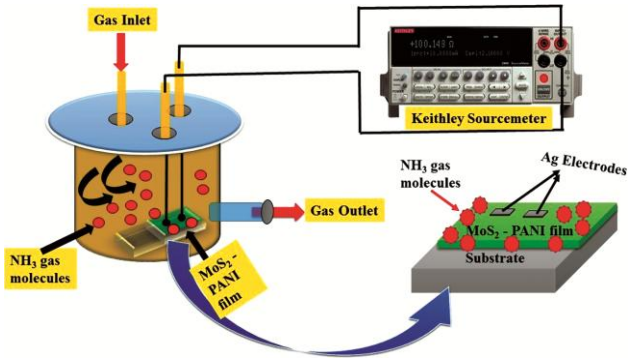

Fig. 1 — Gas sensing set-up for measuring the change in resistance.

3.2 FTIR Study

FTIR results carried out on the samples are shown in Fig. 3. The characteristic transmittance bands near 815 and 1133 cm^{-1} are due to C-H out-of-plane bending vibration and C-H in-plane bending vibration of the benzenoid unit in PANI structure, respectively. The characteristic band at 1298 cm^{-1} corresponds to the C-N stretching mode of the benzenoid unit, which also confirms the conducting nature of doped PANI [36-40]. The bands near 1468 and 1574 cm^{-1} correspond to the C=C and C=N stretching modes of vibrations of benzenoid and quinonoid segments of PANI,

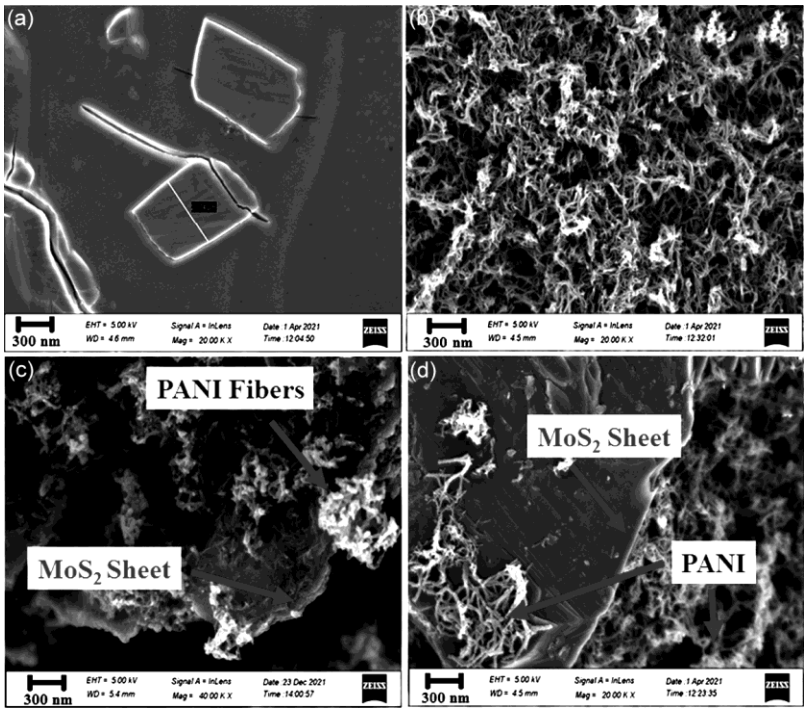

Fig. 2 — FESEM images of (a) MoS_2, (b) PANI, and (c, d) MoS_2-PANI nanocomposite.

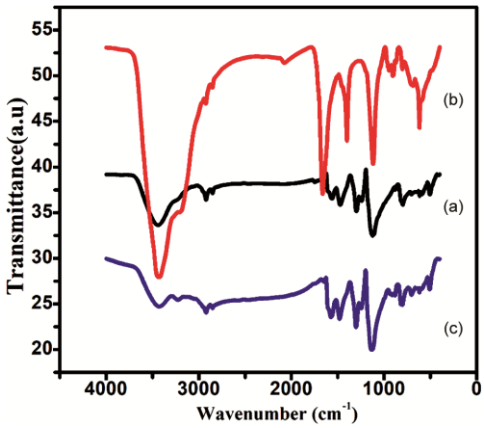

Fig. 3 — FTIR images of PANI (a), MoS_2 (b) and MoS_2-PANI (c) nanocomposites.

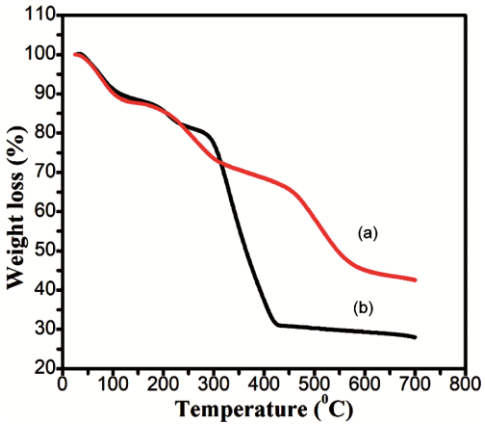

Fig. 4 — TGA thermographs of PANI (a) and MoS_2-PANI (b) nanocomposites.

respectively. These relatively lower frequency bands of benzenoid and quinoid ring stretching are possibly due to the salt formation with HCl[41,42]. The peak at 3424 cm^{-1} is assigned to N-H stretching vibration of the amino group in PANI[43]. The major characteristic peak observed in MoS_2 FTIR spectra at 3439 cm^{-1} is assigned to O-H stretching mode[44]. All the major characteristic peaks of PANI and MoS_2 are also seen in the MoS_2-PANI composite. In addition, an extra peak appears at 914 cm^{-1} in the composite, which is due to the interaction of MoS_2 with PANI. So, one can say that the FTIR result gives evidence of the successful synthesis of the PANI-MoS_2 composites.

3.3 Thermal studies

Knowledge of the thermal stability of PANI is very much important at different thermal conditions in order to visualise its various practical applications. Thermo gravimetric provides information regarding the stability and composition of the sample. Fig. 4. shows TGA plots of PANI and the composites. From the figure, weight loss is evident in three steps for both samples. The first weight loss at around 40-130 °C is due to the evaporation of water content and/or the presence of unreacted monomer in the polymer matrix. Second weight loss at the temperature range of 140-240 °C may be due to the removal of doped ions [45-47]. TGA plot shows maximum weight loss after 240 °C onwards, which might be due to the decomposition of the PANI structure. But in the composites, there is very little weight loss beyond 400 °C compared to bare PANI, and hence it can be concluded that MoS_2-PANI composite has better thermally stability.

TGA data can be utilised to calculate kinetic parameters of a thermal decomposition reaction such as pre-exponential factor, order of reactions and activation energy. In the present study, to calculate the activation energy Coats and Red fern model is followed[48,49] for one-dimensional diffusion is employed, which can be expressed mathematically as

$$ln\left[\frac{g(\alpha)}{T^2}\right. = \ln\left[\frac{AR}{\beta E}\right. \; 1-\frac{2RT}{E} \quad -\frac{E}{RT} \qquad \ldots (1)$$

Where A is the pre-exponential factor, E is the activation energy, and T is the reaction temperature. g(α) is seen to depend on α, the conversion rate. For one dimensional diffusion, $g(\alpha) = \alpha^2$.

The slope and intercept of the plot of $ln\left[\frac{g(\alpha}{T^2}\right.$ vs 1/T give, respectively, the thermal activation energy and the pre-exponential factor. The calculated activation energy obtained from the slope of the plot is around 11.6 KJ/mol for PANI and 25.5 KJ/mol for MoS_2-PANI composite, respectively. The increase in apparent activation energy in MoS_2-PANI composites compared to bare PANI might be due to the interaction between PANI and MoS_2. Once again, it can be said that the PANI-MoS_2 composite is thermally more stable than pure PANI.

3.4 Gas Sensing Studies

Gas sensing measurement of theMoS_2-PANIcomposite is carried out at RT (300 K) for different gases, such as NH_3, methanol (CH_3OH), ethanol (C_2H_5OH) and acetone (C_3H_6O), by measuring the change in electrical resistance of the material on gas intake. Generally, it is believed that the gas-sensing behaviour of any material is a complex phenomenon, and it depends on various parameters, for example, the particle size of the materials, surface morphology, speed of reaction of

gas molecules with the surface molecules and film thickness, *etc*[50,51]. The change of electrical conductivity/resistivity of any material due to non-uniform adsorption and desorption of gas molecules into the surface of the material is measured in terms of sensitivity (S%). In the present work, a detailed study of the effect of MoS_2 2D nanosheet on the NH_3 gas sensing performance of PANI is done. The environmental effect, such as moisture or water content, has been removed by drying the materials meticulously and dehumidifying the test chamber with an ample amount of dehydrating agent within it. The obtained sensitivity of the composite material is observed to be better compared to that of pure PANI and MoS_2, which will be discussed in the second next subsection to follow. Apart from NH_3 sensing, incorporating MoS_2 into PANI is also seen to alter other properties of PANI.

3.4.1 Selectivity Study of MoS_2-PANI Nanocomposite Sensor

Selectivity is an important parameter of a gas sensor and is defined as how it responds to a particular gas in the presence of other gases. The selectivity measurement of a sensor is done in terms of the selectivity coefficient, which is defined in eq.[28]

$$K = \frac{S_A}{S_B}$$

Here, S_A and S_B denote sensitivity towards the most responded gas, NH_3 and other gases, respectively. The selectivity responses of the MoS_2-PANI composite sensor towards various target gases are illustrated in Fig. 5. MoS_2-PANI nanocomposite sensor shows more selectivity towards NH_3 compared to methanol, acetone and ethanol $\left(S_{NH_3}/S_{CH_3OH} = 20, S_{NH_3}/S_{C_3H_6O} = 36, S_{NH_3}/S_{C_2H_5OH} = 44\right)$.

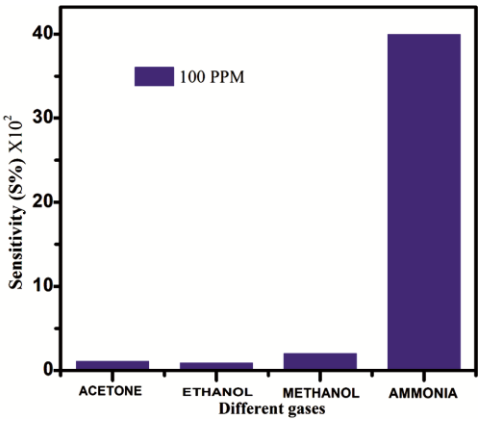

Fig. 5 — Selectivity of the MoS_2-PANI sensor towards various gases.

This indicates better selectivity of the as-prepared sensor towards ammonia vapour with respect to the three other vapours. Detailed gas response and recovery transient studies are done for most responded ammonia gas in the next subsection.

3.4.2 Gas Sensitivity Performance

To calculate the responses of the sensors, the change in electrical resistance is measured both in air and in NH_3. The sensitivity of the sensor is calculated by measuring the change in resistance on gas intake and is defined as in eq.[28]

$$S = (R_{gas} - R_{air})/R_{air} * 100\% \quad \ldots (2)$$

Here, R_{gas} corresponds to the resistances of different concentrations of gases and R_{air} in the fresh air, respectively. Fig. 6 (a, b & c) shows the room temperature sensitivity of the sensors based on pure MoS_2, MoS_2-PANI hybrid and pure PANI sensors for different concentrations (20−100 ppm) of NH_3 gas, respectively. For both PANI and MoS_2-PANI sensors, the sensitivity follows increased trends with the increase in NH_3 concentration. However, for 100 ppm concentration, the order of sensitivity of the

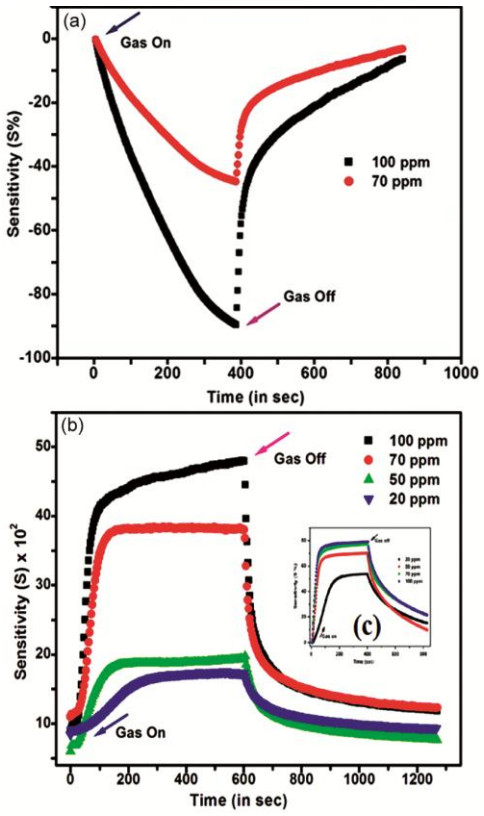

Fig. 6 — Room temperature transient responses of the (a) MoS_2, (b) MoS_2-PANI composite, and the inset in (b) shows results for bare PANI(c) [28] sensor towards different NH_3 concentrations.

composite is two orders of magnitude more than that of pure PANI; so, to say, the change in film resistance is found to be two orders more in the composite film. For all the concentrations of NH_3 gas, resistance increases to a peak value and saturates within a few seconds upon exposure to NH_3 vapour and fully recovers on the withdrawal of the gas. However, for pure MoS_2, the response of the film is found to decrease for 70 and 100 ppm only. This means NH_3 gas acts as electron donor, transferring electrons to the conduction band of MoS_2, leading to increased electron concentration and conductivity[52]. Pure MoS_2 film does not show any response below 50 ppm towards NH_3 gas. A comparative gas sensing results on the study of the present MoS_2-PANI composite with some works available in the literature on similar materials carried out by some other research groups is shown in Table 1.

3.4.3 Sensor Response and Recovery Time

Response and recovery times are considered essential parameters to recognise a good sensor, as these parameters depend upon the adsorption and desorption rate of sensors. Response and recovery times of ideal sensors are defined as the time to change its basic states up to 90% of its maximum saturated value on gas intake and the time it is 10% near its basic state in the absence of gas, respectively[56,57]. The response and recovery plots of pure MoS_2 and the MoS_2-PANI nanocomposites are shown in Fig. 7 (a & b).The response and recovery time for pure MoS_2 found to be 370 and 412 s, and 382 and 386 for 70 ppm and 100 ppm, respectively. The pure MoS_2 film does not respond to lower concentrations (20 and 50 ppm) of NH_3. Also, for MoS_2-PANI nanocomposite film, the response time varies from 95 to 45 s and recovery time from 90 to 30 s with the increase in NH_3 concentration.

3.4.4 Repeatability, Limit of Detection and Stability of MoS_2-PANI Sensor

Repeatability, the limit of detection (LOD) and long-term stability are imperative parameters of a gas sensor as it determines the reliability of the gas sensor. For repeatability measurement, the gas chamber is repeatedly injected and evacuated for a duration of 15 min. Fig. 8(a) shows a repeatability plot for the MoS_2 -PANI sensors, which is done for a fixed concentration of NH_3 and studied for three successive cycles. The study reveals very less variation in respective gas response, which makes an indication about the stability of the sensor working at RT. The detection limit (LOD) of the MoS_2-PANI sensor is evaluated using the following eq.[57]

$$LOD = {}^{(3.0 * \sigma)}/_{S} \quad \ldots (3)$$

Table 1 — Comparison of the sensing performance of the MoS_2-PANI sensor in this work with other previously reported NH_3 sensors.

Materials	S (%)	t_{res} (Sec)	t_{rec} (Sec)	Operating temperature	Detected Gas	DR	Reference
SnO_2/PANI	16 (500 ppm)	12-15	80	RT	Ammonia	(100-500) ppm	[53]
PANI/TiO_2	5.55 (117 ppm)	18	58	25°C	Ammonia	(23–141) ppm	[54]
PANI/ MoS_2 / SnO_2	10.9(100ppm)	21	130	RT	Ammonia	(500 ppb-100ppm)	[59]
PANI/MWCNTs/MoS_2	11 (250 ppb)	32	36	RT	Ammonia	0.25 ppm	[34]
PANI-ZnO	4.6 (20 ppm)	153	135	RT	Ammonia	(20-100) ppm	[55]
PANI/CdS	250% (100ppm)	96-58	127-104	RT	Ammonia	(20-100) ppm	[28]
PANI/MoS_2	40 x 10^2 (100 ppm)	95-45	90-30	RT	Ammonia	(20-100) ppm	Present work

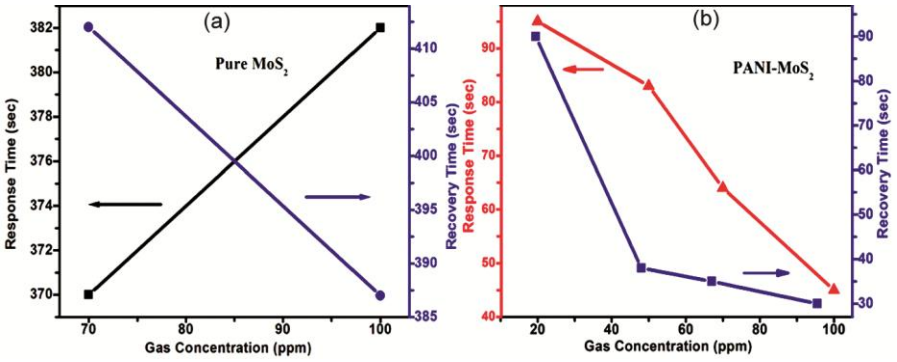

Fig. 7 — The response and recovery times of (a) MoS_2 and (b) MoS_2-PANI nanocomposite for different concentrations (20-100 ppm) of NH_3 gas.

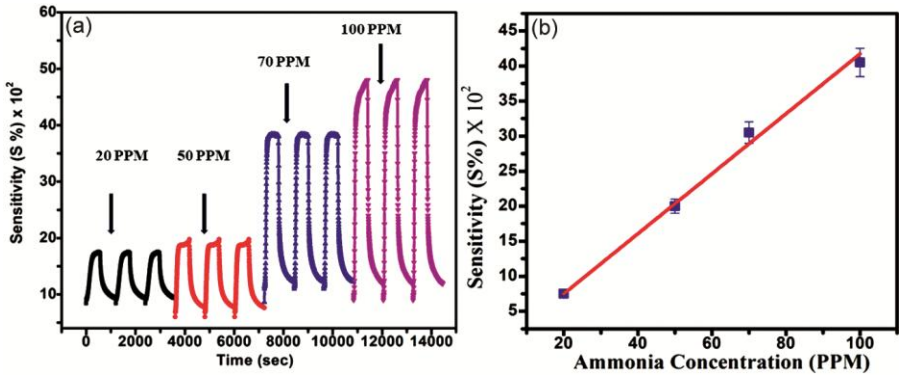

Fig. 8 (a) — Repeatability plot of MoS_2-PANI sensor for different NH_3 concentrations; (b) — Sensitivity vs ammonia concentration of the MoS_2-PANI sensor.

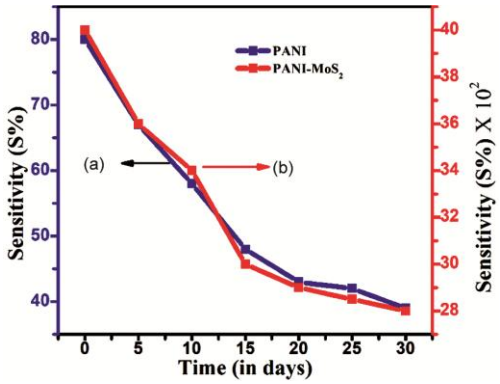

Fig. 9 — Sensitivity vs ageing plots for PANI (a) and MoS_2-PANI (b) composite sensor.

Where σ and S refer to the relative standard deviation and slope of the calibration curve. The nature of the variation is shown in Fig. 8(b), and its value is obtained as 10 ppm. To investigate the ageing nature of these sensors, the stability performance is measured for 30 days at regular intervals of 5 days. Fig. 9 shows the observed gas sensitivity of MoS_2-PANI, and the observed changes are not very large, which demands that the prepared room temperature operated sensor has long-term stability. From this curve, the PANI-MoS_2 composite showed better results (70%) compared to PANI (48%). So, it may be claimed that the PANI decorated MoS_2 sensor shows comparatively better stability compared to its counterpart of the bare PANI sensor. Overall, the authors are tempted to claim that with excellent selectivity, sensitivity, repeatability, and low fabrication cost, the MoS_2-PANI composite sensor is a promising candidate for detecting NH_3 at room temperature. So, with proper improvisation, this sensor can be utilised for numerous applications in industrial and domestic areas.

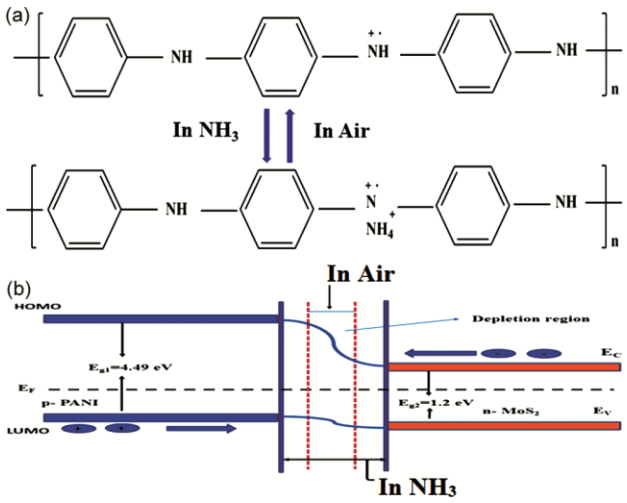

Fig. 10 — Schematic of ammonia sensing mechanism of PANI and MoS_2-PANI sensor from chemical (a) and band diagram (b) point of view.

3.4.5 Gas Sensing Mechanism

The gas sensing mechanism of PANI and MoS_2-PANI sensor has been described in Fig. 10 (a & b). Conventionally PANI is known to exist in the two most useable states, the conducting emeraldine salt (ES) and insulating emeraldine base (EB) forms and in suitable reversible doping/developing processes, both states are converted to vice-versa. For bare PANI sensors, the response is generally based on the process of protonation and deprotonation arising from the adsorption/desorption of NH_3 on the surface.

PANI, in its ES form, gains proton to form (N^+-H) bonds or abundant active sites due to in-situ chemical oxidative polymerization[34]. On exposure to NH_3, the N-H group of PANI (ES) react with ammonia vapour molecules to produce N-H_4^+(ammonium ion) and transform PANI to its insulating EB form resulting in the increase of resistance[8,58,59]. On withdrawal of NH_3,

the ammonium ion is decomposed to NH_3(gas) along with the release of a proton, and the PANI sensor regains its original state of ES. The involved reversible reaction in the process can be written as[60]

$$NH_3(gas)+PANI\text{-}NH^+ \leftrightarrow PANI + NH_4^+.$$
$$NH_4^+ \xrightarrow{\text{In Air}} NH_3(gas) + H^+$$

The composite nanosheets of MoS_2 provide a larger surface area, which adds further in providing a larger surface area to facilitate more ammonia adsorption[34].

The sensing can also be explained from another perspective of depletion layer alteration formed in the heterojunction. PANI is known to behave as a p-type semiconductor and MoS_2as an n-type one[59]. Therefore, there is a possibility of the formation of p-n heterojunctions at a microscopic level between PANI and MoS_2, which may be another factor responsible for the NH_3 sensing of MoS_2-PANI film[61,62]. The energy band diagram for PANI and MoS_2 is shown in Fig. 10(b). A depletion region is assumed to form at the interface between p-type PANI and n-type MoS_2 due to the carrier concentration gradient between them until an equilibrium condition is reached[61]. On exposure to NH_3, the protons from the PANI side would be captured by the gas molecules, causing the lowering of the density of the hole in PANI[59], which results in the widening of the depletion region and hence a decrease of the self-established electric field. Therefore, charge transfer is restricted between PANI and MoS_2 and subsequently increases in the resistance to gas intake.

4 Conclusions

An ammonia sensor based on PANI decorated 2-D MoS_2nanosheets using a simple chemical in-situ polymerisation technique has been successfully developed. The morphology, thermal stability and elemental compositions of the materials, as manifested from FESEM, TGA and FTIR, show compatible results. The designed MoS_2-PANI sensor exhibit fair response-recovery time, excellent reproducibility and selectivity. The sensitivity of the composite sensor is two orders of magnitude more compared to that of bare PANI towards 100 ppm NH_3 at room temperature. The results on the structure, stability, and excellent gas sensing properties might lead it as a promising material to detect hazardous NH_3 in ambient conditions.

Acknowledgements

The authors thank UGC (Project grant no. 40-458/2011 (SR), Department of Science and Technology (Project grant no. DST/TSG/PT/2009/96) for providing instrumentation facilities and DST (FIST) for minor equipment. Thanks are also to SAIF Gauhati University for TGA measurements, CIF Gauhati University for FESEM measurements, and CIF Tezpur University for FTIR measurements.

Declaration

Authors state that there is no conflict of interest among the authors, and also, all funding agencies are duly acknowledged. All authors declare that they have no competing financial interests.

References

1 Yang H, Ma S, Jiao H, Chen Q, Lu Y, JinW, Li W, Wang T, Jiang X, Qiang Z & Chen H, *Sens Actuators* B, 245 (2017) 493.
2 Fedoruk M J, Bronstein R & Kerger B D, *J Exposure Anal Environ Epidomiol*, 15 (2005) 534.
3 Diana M, Roekmijati W & Suyud W, *EDP Sci*, 73 (2018) 06003.
4 Bardocz S, *Trends Food Sci Technol*, 6 (1995) 341.
5 Hurtado J L & Lowe C R, *ACS Appl Mater Interfaces*, 6 (2014) 8903.
6 Mani G K & Rayappan J B B, *Mater Sci Eng B Solid-State Mater Adv Technol*, 191 (2015) 41.
7 Timmer B, Olthuis W & Berg A V D, *Sens Actuators B*, 107 (2005) 666.
8 Abdulla S, Mathew T L & Pullithadathil B, *Sens Actuators B*, 221 (2015) 1523.
9 Mikhaylov S, Ogurtsov N, Noskov Y, Redon N, Coddeville P, Wojkiewicz J L & Pud A, *RSC Adv*, 5 (2015) 20218.
10 Eising M, Cava C E, Salvatierra R V, Zarbin A J G & Roman L S, *Sens Actuators B*, 245 (2017) 25.
11 Santos M C, Bianchi A G C, Ushizima D M, Pavinatto F J & Bianchi R F, *Sens Actuators B*, 253 (2017) 156.
12 Wua S, Zeng F, Li F & Zhu Y, *Eur Polym J*, 36 (2000) 679.
13 Pandey S, *J Sci: Adv Mater Dev*, 1 (2016) 431.
14 Janata J & Josowicz M, *Nat Mater*, 2 (2003) 19.
15 Capone S, Siciliano P, Quaranta F, Rella R, Epifani M & Vasanelli L, *Sens Actuators B*, 69 (2000) 230.
16 TsujitaW, Yoshino A, Ishida H&MoriizumiT, *Sens Actuators* B, 110 (2005) 304.
17 Barsan N, Koziej D & Weimar U, *Sens Actuators* B, 121 (2007) 18.
18 Zhang D, Sun Y, Li P & Zhang Y, *ACS Appl Mater Interfaces*, 8 (2016) 14142.
19 Zhao P X, Tang Y, Mao J, Chen Y X, Song H, Wang J W, Song Y, Liang Y Q & Zhang X M, *J Alloys Compd*, 674 (2016) 252.
20 Zhang D, Jiang C & Sun Y, *J Alloys Compd*, 698 (2017) 476.
21 Baek D & Kim J, *Sens Actuators B*, 250 (2017) 686.
22 Niu Y, Jiao W C, Wang R G, Ding G M & Huang Y F, *J Mater Chem* A, 4 (2016) 8198.
23 Donarelli M, Prezioso S, Perrozzi F, Bisti F, Nardone M, Giancaterini L, Cantalini C & Ottaviano L, *Sens Actuators B*, 207 (2015) 602.

24 Liu Y, Hao L, Gao W, Wu Z, Lin Y, Li G, Guo W, Yu L, Zeng H, Zhu J & Zhang W, *Sens Actuators* B, 211 (2015) 537.
25 Lee E, Yoon Y S & Kim D J, *ACS Sens*, 3 (2018) 2045.
26 Kulkarni S B, Navale Y H, Navale S T, Stadler F J, Ramgir N S & Patil V B, *Sens Actuators B*, 288 (2019) 279.
27 Bandgar D K, Navale S T, Naushad M, Mane R S, Stadler F J & Patil V B, *RSC Adv*, 5 (2015) 68964.
28 Akbar A, Das M & Sarkar D, *Sens Actuators* A, 310 (2020) 112071.
29 Ye Z, Jiang Y, Tai H, Guo N, Xie G & Yuan Z, *J Mater Sci: Mater Electron*, 26 (2015) 833.
30 Xu L H & Wu T M, *J Mater Sci: Mater Electron*, 31 (2020) 7276.
31 Harale N S, Nagare A B, Mali S S, Suryawanshi M P, Sharma K K K, Rao V K, Hong C K, Kim J H & Patil P S, *J Electron Mater*, 49 (2020) 1338.
32 TohidiT S & Mohammad-Rezaei R, *J Mater Sci: Mater Electron*, 31 (2020) 19119.
33 Wang X, Meng S, Tebyetekerwa M, Weng W, Pionteck J, Sun B, Qin Z & Zhu M, *Synth Met*, 233 (2017) 86.
34 Zhang D, Wu Z, Li P, Zong X, Dong G & Zhang Y, *Sens Actuators B*, 258 (2018) 895.
35 Vattikuti S V P & Byon C, *J Nanomater*, 2015 (2015) 1.
36 Lu X, Hu Y, Li W, Guo Q, Chen S, Chen S, Hou H & Song Y, *Electrochim. Acta*, 189 (2016) 158.
37 Oraon R, De Adhikari A, Tiwari S K & Nayak G C, *RSC Adv*, 5 (2015) 68334.
38 Majumder M, Choudhary R B, Thakur A K & Karbhal I, RSC Adv, 7 (2017) 20037.
39 Khan A A & Khalid M, *Synth Met*, 160 (2010) 708.
40 Das M, Akbar A & Sarkar D, *Synth Met*, 249 (2019) 69.
41 Stejskal J, Sapurina I, Prokes J & Zemek J, *Synth Met*, 105 (1999) 195.
42 Arasi A Y, Jeyakumari J J L, Sundaresan B, Dhanalakhsmi V & Anbarasan R, *Spectrochim Acta A*, 74 (2009) 1229.
43 Shaban M, Rabia M, Abd El-Sayed A M, Ahmed A & Sayed S, *Sci Rep*, 7 (2017) 14100.
44 Huang K J, Wang L, Liu Y J, Liu Y M, Wang H B, Gan T & Wang L L, *Int J Hydrog Energy*, 38 (2013) 14027.
45 Roy S, Saxena S K, Yogi P, Pathak D K, Chaudhary A & Kumar R, *Adv Mater Process Technol*, 5 (2019) 172.
46 Swati, Saini M, Anupama & Shukla R, *Ceram Int*, 47 (2021) 33835.
47 Baba Z M, *J Appl Polym Sci*, 113 (2009) 3980.
48 Kahrizsangi R E & Abbasi M H, *Trans Nonferrous Met Soc China*, 18 (2008) 217.
49 Wu X, Liu M & Jia M, *Synth Met*, 185 (2013) 145.
50 Chakraborty S & Pal M, *Sens Actuators B*, 242 (2017) 1155.
51 Gurav K V, Gang M G, Shin S W, Patil U M, Deshmukh P R, Agawane G L, Suryawanshi M P, Pawar S M, Patil P S, Lokhande C D, Kim J H, *Sens Actuators B*, 190 (2014) 439.
52 Park J, Mun J, Shin J S & Kang S W, *R Soc Open Sci*, 5 (2018) 181462.
53 Deshpande N G, Gudage Y G, Sharma R, Vyas J C, Kim J B & Lee Y P, *Sens Actuators B*, 138 (2009) 76.
54 Tai H, Jiang Y, Xu G, Yu J & Chen X, *Sens Actuators B*, 125 (2007) 644.
55 Patil S L, Chougule M A, Pawar S G, Sen S, Moholkar A V, Kim J H & Patil V B, *Sens Transducers*, 134 (2011) 120.
56 Mukherjee K, Majumder S B, *J Appl Phys*, 106 (2009) 064912.
57 Das M & Sarkar D, *Ceram Int*, 43 (2017) 11123.
58 Fan G, Chen D, Li T, Yi S, Ji H, Wang Y, Zhang Z, Shao G, Fan B, Wang H, Xu H, Lu H, Zhou Y, Zhang R & Sun J, *Sens Actuators B*, 312 (2020) 127892.
59 Liu A, Lv S, Jiang L, Liu F, Zhao L, Wang J, Hu X, Yang Z, He J, Wang C, Yan X, Sun P, Shimanoe K & Lu G, *Sens Actuators* B, 332 (2021) 129444.
60 Wang X, Gong L, Zhang D, Fan X, Jin Y & Guo L, *Sens Actuators B*, 322 (2020) 128615.
61 Zhang D, Chang H, Sun Y, Jiang C, Yao Y & Zhang Y, *Sens Actuators B*, 252 (2017) 624.
62 Ullah H, Shah A, Bilal S & Ayub K, *J Phys Chem* C, 117 (2013) 23701.